

RESEARCH PAPER

Spermidine-enhanced autophagic flux improves cardiac dysfunction following myocardial infarction by targeting the AMPK/mTOR signalling pathway

Jing Yan^{1,2,3} | Jian-Yun Yan^{1,2,3}  | Yu-Xi Wang^{1,2,3} | Yuan-Na Ling^{1,2,3} |
 Xu-Dong Song^{1,2,3} | Si-Yi Wang^{1,2,3} | Hai-Qiong Liu^{1,2,3} | Qi-Cai Liu^{1,2,3} | Ya Zhang⁴ |
 Ping-Zhen Yang^{1,2,3} | Xian-Bao Wang^{1,2,3} | Ai-Hua Chen^{1,2,3} 

¹Laboratory of Heart Center and Department of Cardiology, Heart Center, Zhujiang Hospital, Southern Medical University, Guangzhou, China

²Laboratory of Heart Center, Guangdong Provincial Biomedical Engineering Technology Research Center for Cardiovascular Disease, Guangzhou, China

³Laboratory of Heart Center, Sino-Japanese Cooperation Platform for Translational Research in Heart Failure, Guangzhou, China

⁴Department of Cardiology, Xiangdong Affiliated Hospital of Hunan Normal University, Zhuzhou, Hunan, China

Correspondence

Ai-Hua Chen, Xian-Bao Wang, and Ping-Zhen Yang, Laboratory of Heart Center and Department of Cardiology, Heart Center, Zhujiang Hospital, Zhujiang Hospital of Southern Medical University, Guangzhou, Guangdong 510000, China.
 Email: chenaha@126.com; wxb2007wx@126.com; y.pingzhen@yahoo.com

Funding information

National Natural Science Foundation of China, Grant/Award Number: No. 81400190 No. 81470488 No. 81873460; Natural Science Foundation of Guangdong Province, Grant/Award Number: No. 2015A030310478 No. 2017A030313703

Background and Purpose: Spermidine, a natural polyamine, is abundant in mammalian cells and is involved in cell growth, proliferation, and regeneration. Recently, oral spermidine supplements were cardioprotective in age-related cardiac dysfunction, through enhancing autophagic flux. However, the effect of spermidine on myocardial injury and cardiac dysfunction following myocardial infarction (MI) remains unknown.

Experimental Approach: We determined the effects of spermidine in a model of MI, Sprague–Dawley rats with permanent ligation of the left anterior descending artery, and in cultured neonatal rat cardiomyocytes (NRCs) exposed to angiotensin II (Ang II). Cardiac function in vivo was assessed with echocardiography. In vivo and in vitro studies used histological and immunohistochemical techniques, along with western blots.

Key Results: Spermidine improved cardiomyocyte viability and decreased cell necrosis in NRCs treated with angiotensin II. In rats post-MI, spermidine reduced infarct size, improved cardiac function, and attenuated myocardial hypertrophy. Spermidine also suppressed the oxidative damage and inflammatory cytokines induced by MI. Moreover, spermidine enhanced autophagic flux and decreased apoptosis both in vitro and in vivo. The protective effects of spermidine on cardiomyocyte apoptosis and cardiac dysfunction were abolished by the autophagy inhibitor chloroquine, indicating that spermidine exerted cardioprotective effects at least partly through promoting autophagic flux, by activating the AMPK/mTOR signalling pathway.

Conclusions and Implications: Our findings suggest that spermidine improved MI-induced cardiac dysfunction by promoting AMPK/mTOR-mediated autophagic flux.

1 | INTRODUCTION

Myocardial infarction (MI) has emerged as a major cause of morbidity and mortality worldwide which not only reduces human life span but

also exerts a heavy burden on health care systems (Murray & Lopez, 1997; Jernberg et al., 2015). Poor prognoses after MI result from adverse cardiac structural changes, deteriorated cardiac function, and irreversible cardiomyocyte death (White et al., 1987). It is well

Abbreviations: AMPK, AMP activated protein kinase; Ang II, angiotensin II; CCK-8, cell counting kit-8; CQ, chloroquine; DCFH-DA, dichlorofluorescein diacetate; HW/BW, heart weight/body weight; LV, left ventricle; LVEF, left ventricular ejection fraction; LVFS, left ventricular fractional shortening; LVIDd, LV internal diameters at diastole; LVIDs, LV internal diameters at systole; MDA, malondialdehyde; MI, myocardial infarction; mTOR, mammalian target of rapamycin; NRCs, neonatal rat cardiomyocytes; PI, propidium iodide; WGA, wheat germ agglutinin

established that activation of the renin-angiotensin system plays a critical role in the pathogenesis of post-MI heart failure. Currently, there is much evidence for the use of ACE inhibitors and angiotensin receptor blockers in the management of heart failure after MI. These agents block the renin-angiotensin system and thus stabilize left ventricle remodelling, relieve patient symptoms, prevent hospitalization, and prolong life (McMurray, 2011). Unfortunately, the prognosis for post-MI heart failure is still unsatisfactory and it is therefore imperative to find more effective drugs or therapeutic targets for treating post-MI cardiac dysfunction and improving patient prognosis.

Spermidine, one of the natural polyamines found in mammalian cells, participates in many cellular processes, under various pathophysiological conditions (Igarashi & Kashiwagi, 2010; Pegg, 2016). Dietary spermidine is absorbed quickly from the intestines (Milovic, 2001), resulting in subsequent increased levels of this polyamine in the blood (Soda et al., 2009). Previous researches have demonstrated that SPD provides potential health benefits (Atiya Ali, Poortvliet, Strömberg, & Yngve, 2011; Zoumas-Morse et al., 2007). However, whether exogenous oral SPD supplements alleviate myocardial injury and improve cardiac function after MI remains unknown.

Recently, inducers of autophagy, such as rapamycin, metformin, and resveratrol, have shown cardioprotective effects after MI (Kanamori et al., 2013; Filippone et al., 2017; D. Sun & Yang, 2017). Spermidine also promotes health by induction of autophagy (Madeo, Eisenberg, Pietrocola, & Kroemer, 2018). Moreover, treatment with spermidine extends lifespan and exerts neuroprotection in an autophagy-dependent manner (Eisenberg et al., 2009; Gupta et al., 2013). Thus, it is reasonable to propose that spermidine-induced autophagy might play a role in decreasing myocardial injury and improving cardiac function post-MI. The **AMP activated protein kinase** (AMPK) is a an enzyme also involved in autophagy (Ha & Kim, 2016). Another kinase, the **mammalian target of rapamycin** (mTOR), is downstream of AMPK and is also involved in the regulation of autophagy (L. Sun et al., 2015). Given its ability to induce autophagy, we have tested the possibility that spermidine might enhance autophagic flux via the AMPK/mTOR signalling pathway in rats post-MI.

2 | METHODS

2.1 | Animal experiments

All animal care and experimental procedures complied with the Guidelines for the Care and Use of Laboratory Animals formulated by the Ministry of Science and Technology of China, and were approved by the Ethics Committee of the Southern Medical University. Animal studies are reported in compliance with the ARRIVE guidelines (Kilkenny, Browne, Cuthill, Emerson & Altman, 2010; McGrath, Drummond, McLachlan, Kilkenny, & Wainwright, 2010) and with the recommendations made by the *British Journal of Pharmacology* (McGrath & Lilley, 2015). The current study is based on the rule of the replacement, refinement, or reduction. The rats were housed

What is already known

- Spermidine is known to induce autophagy and exhibits protective effects against age-related diseases.

What this study adds

- Spermidine exerted cardioprotective effects against MI by promoting autophagic flux through the AMPK/mTOR signalling pathway.

What is the clinical significance

- It is imperative to find more effective drugs for treating post-MI cardiac dysfunction.
- Pharmacological intervention with spermidine may be a promising treatment for patients with MI.

under standard laboratory conditions with a light/dark cycle of 12 hr and had free access to sufficient food and water. Male Sprague–Dawley rats (200–220 g; RRID:MG1:5651135) were used to model MI by permanent ligation of the left anterior descending artery, as previously described (Cheng et al., 2012). Briefly, rats were anaesthetized with pentobarbital sodium (40 mg·kg⁻¹; Sigma-Aldrich, St. Louis, MO, USA), given by intraperitoneal injection. A mini-ventilator (Taimeng, Chengdu, China) was used to maintain gas exchange in the lungs by endotracheal tube. After the heart had been exposed, the left anterior descending artery was permanently ligated (except in the sham group). Then after the arterial occlusion, the rats were randomly divided into the different experimental groups.

Rats received the following treatments for 4 weeks: (a) Sham group was given normal drinking water; (b) MI group also received normal drinking water; (c) MI + SPD group was given drinking water containing spermidine (5 mM, Sigma-Aldrich); (d) MI + SPD + **chloroquine** (CQ; Sigma,) group was given drinking water treated with spermidine (5 mM) and daily intraperitoneal injections of CQ (50 mg·kg⁻¹ per day); (e) MI + CQ group was given normal drinking water and intraperitoneal injections of CQ (50 mg·kg⁻¹ per day); (f) MI + SPD + **Compound C** group was given drinking water with SPD (5 mM) and intraperitoneal injections of Compound C (20 mg·kg⁻¹ for 3 days; Selleck, Houston, TX, USA). Administration of spermidine in drinking water has been described elsewhere (Michiels, Kurdi, Timmermans, De Meyer & Martinet, 2016). The rats in each group were checked daily for 4 weeks after induction of MI, for survival analysis. At the indicated time point, the rats were killed and the heart tissues collected for later analysis. The in vivo experimental protocol is shown in Figure 1a.

2.2 | Cardiomyocyte isolation and culture

Neonatal rat cardiomyocytes (NRCs) were isolated from 1- to 2-day-old Sprague–Dawley rats, as described by Gottlieb & Gustafsson (2011). NRCs were incubated at 37°C in a 5% CO₂ atmosphere. First,

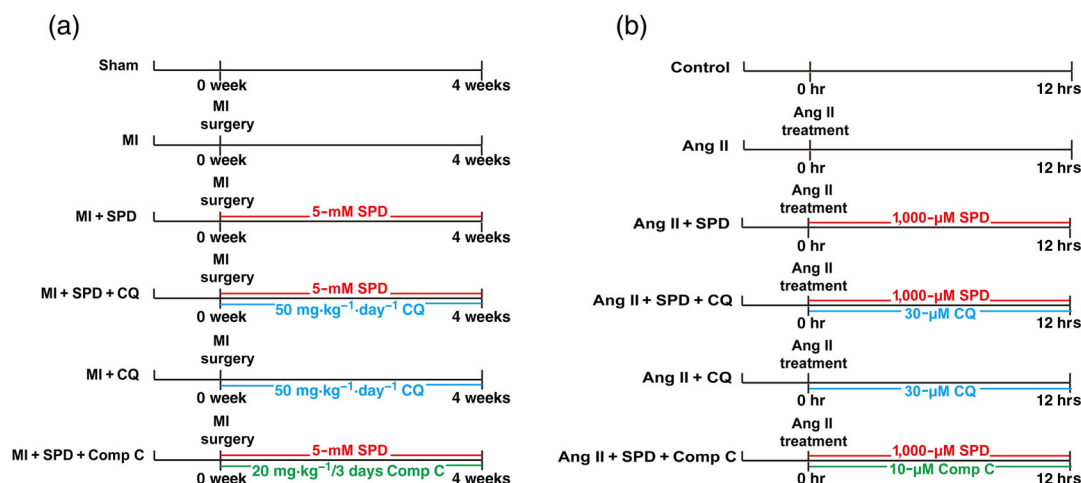


FIGURE 1 (a) Experimental protocol of the in vivo study. (b) Experimental protocol of the in vitro study

cells were cultured in DMEM containing 10% horse serum for 60 hr. Then, cells were cultured in serum-free medium 12 hr for starvation. After 72-hr incubation, these cells were randomly divided into the following treatment groups: (a) control group; (b) **angiotensin II** (Ang II) group, NRCs exposed to Ang II (1 μM) to stimulate cardiomyocyte injury; (c) Ang II + SPD group, treated with Ang II (1 μM) and spermidine (1,000 μM); (d) Ang II + SPD + CQ group treated with Ang II (1 μM), spermidine (1,000 μM), and CQ (30 μM); (e) Ang II + CQ group treated with Ang II (1 μM) and CQ (30 μM); (f) Ang II + SPD + Compound C group treated with Ang II (1 μM), spermidine (1,000 μM), and Compound C (10 μM). After 12-hr incubation with the different treatments, the NRCs were harvested and prepared for analysis. The in vitro experimental protocol is shown in Figure 1b.

2.3 | Cell viability assay

Viability of NRCs was measured using a CCK-8 assay kit (MCE, NJ, USA) according to the manufacturer's instructions. Briefly, NRCs were seeded in 96-well plates and followed by the different treatments at indicated times. Then, the NRCs were incubated with 10-μl CCK-8 reagent in the dark for 4 hr. Absorbance was measured at 450 nm using a microplate reader (Thermo, NY, USA), and the readings were normalized by comparison with vehicle control.

2.4 | Propidium iodide staining

Propidium iodide (PI) staining was performed using a PI staining kit (Yeasen, Shanghai, China). Briefly, the NRCs were incubated in laser confocal dishes. Then, the cells were harvested and were washed with PBS three times. PI staining solution was incubated with the cells for 15 min, followed by counterstaining with Hoechst 33342 solution. Then, images were taken under a fluorescence microscope.

2.5 | Western blot

The antibody-based procedures used in this study comply with the recommendations made by the *British Journal of Pharmacology* (Alexander et al., 2018). Rat hearts and the isolated NRCs were lysed in RIPA buffer. The protein concentrations were then measured by BCA protein assay kits (Thermo Scientific). Protein was separated by SDS-PAGE and transferred to a PVDF membrane, followed by incubation with 5% non-fat milk blocking buffer for 2 hr. Membranes were then incubated with the following primary antibodies at 4°C overnight: anti-LC3 B (CST cat#: 2775S RRID:AB_915950), anti-p62 (CST cat#: 5114S RRID:AB_10624872), anti-caspase-3 (CST cat#: 9662S RRID:AB_331439), anti-Bcl-2 (CST cat#: 2876S), anti-Bax (CST cat#: 2772S RRID:AB_10695870), anti-p-AMPK (CST cat#: 2535S RRID:AB_331250), anti-AMPK (CST cat#: 2532S RRID:AB_330331), anti-p-mTOR (CST cat#: 5536S RRID:AB_10691552), anti-mTOR (CST cat#: 2972S RRID:AB_330978), and anti-GAPDH (1:10,000, Boster cat#: AP0063 RRID:AB_2651132). The membranes were incubated with secondary antibodies (1:8,000, Boster, Shanghai, China) and visualized by ECL kits (Engreen, Beijing, China). The levels of protein were quantified using Image Pro-Plus 6.0 software (RRID:SCR_016879) and were normalized to control.

2.6 | Assessment of myocardial infarct size

Masson-trichrome staining was used to detect the myocardial fibrosis that marked the ventricular infarct zones in the different groups of rats. The myocardial tissues were fixed in 4% paraformaldehyde after the rats were killed. The samples were then processed by standard histological techniques, being dehydrated in increasing concentrations of ethanol, transferred to xylene, and then embedded in paraffin. Heart samples were cut into 6-μm sections on a microtome, and then deparaffinized, followed by Masson's trichrome staining. The infarcted region, identified by replacement of cardiomyocytes by fibrotic tissue, was stained blue. The images were captured by a light microscope.

2.7 | Echocardiography

Echocardiography was performed using a Vevo 2100 System equipped with a 30-MHz transducer (Fujifilm Visual Sonics, Inc., Toronto, Canada). Rats were anaesthetized with 2% isoflurane, and the left chest was denuded using depilatory cream. M-mode echocardiographic examinations of the short axis were obtained. The left ventricular (LV) fractional shortening (LVFS), LV ejection fraction (LVEF), LV internal diameters at diastole (LVIDd), LV internal diameters at systole (LVIDs), LV anterior wall thickness at diastole, LV anterior wall thickness at systole, LV posterior wall thickness at diastole, and LV posterior wall thickness at systole were calculated.

2.8 | Heart weight/body weight measurement

Rats were weighed and killed 4 weeks after MI, and the hearts were collected and fixed in 4% paraformaldehyde overnight. The weight of hearts was measured, and heart weight/body weight (HW/BW) ratio was calculated. The whole hearts in different groups were photographed.

2.9 | Wheat germ agglutinin staining

Heart tissues were fixed in 4% paraformaldehyde, dehydrated in ethanol, cleared in xylene, and embedded in paraffin. Samples were then cut into 6- μ m sections on a microtome and deparaffinized. To measure surface area of cardiomyocytes, cardiac sections were stained with wheat germ agglutinin (WGA) solution according to the manufacturer's instructions. After that, sections were imaged using a fluorescence microscope. Green fluorescence indicates cell membrane, and surface area of cardiomyocytes was analysed by ImageJ software (RRID:SCR_003070).

2.10 | Intracellular ROS measurements in NRCs

ROS were measured by 2,7-dichlorofluorescein diacetate (DCFH-DA; Solarbio, Beijing, China) according to the manufacturer's instructions. Briefly, NRCs were incubated with 10-nM DCFH-DA for 20 min at 37°C, followed by counterstaining with Hoechst 33342 solution. Then, NRCs were washed three times with PBS. Cells were visualized by fluorescence microscopy.

2.11 | Determination of SOD activity and malondialdehyde levels

Heart tissues were collected at the indicated time points from the different groups and homogenized. SOD activity was measured using a SOD detection kit (Beyotime, Shanghai, China), and malondialdehyde (MDA) content was detected by an MDA kit (Beyotime, Shanghai, China) according to the manufacturer's instructions. The OD value was measured at 450- and 532-nm wavelengths, respectively, by a microplate reader.

2.12 | Measurement of inflammatory cytokines

The cardiac tissues were collected at the indicated time points from the different groups of rats and homogenized. The level of inflammatory cytokines including **TNF- α** , **IL-1 β** , and **IL-6** were measured by ELISA kits (MSK, Wuhan, China) according to the manufacturer's protocol. The absorbance was measured at 450 nm using a microplate reader.

2.13 | Apoptosis assay

Apoptosis was analysed applying a TUNEL assay kit (Beyotime, Shanghai, China) according to the manufacturer's protocol. TUNEL assays were visualized with light microscopy or fluorescent microscopy. TUNEL-positive nuclei were stained green in fluorescence images and stained brown in histological images. TUNEL-stained cells (%) were calculated according to the distribution of cardiomyocytes by captured images.

2.14 | Evaluation of fluorescent LC3 puncta

The NRCs were seeded in confocal dishes and were transfected with adenovirus encoding tandem fluorescent mRFP-GFP-LC3 (MOI = 15). At the indicated times, cells were randomly divided into groups, according to the different treatments described above. After treatment, cells were washed with PBS and then fixed with 4% paraformaldehyde and counterstained with DAPI. Cells were viewed and photographed under a confocal laser scanning microscope (Carl Zeiss, Germany). Punctuate localization of LC3 on autophagosomes had both red and green fluorescence and appeared yellow in merged images, indicating autophagosome. Subsequently, GFP in the acidic pH of the lysosome is unstable and loses the green fluorescent signal in the fused autophagosome-lysosomes. Consequently, red dots that do not overlap green dots in merged images indicate autolysosome formation. The numbers of autophagosomes (yellow dots) and autolysosomes (red dots) and the ratio of autophagosomes/autolysosomes was measured.

2.15 | Immunohistochemistry

Heart tissues were fixed in 4% paraformaldehyde, dehydrated in ethanol, cleared in xylene, and embedded in paraffin. Samples were then cut into 6- μ m sections on a microtome and deparaffinized. Sections were blocked with 1% BSA at room temperature for 30 min and incubated with specific primary antibodies at 4°C overnight, including anti-p62 (Servicebio cat#: GB11239), anti-LC3B (Servicebio cat#: GB11124), anti-p-AMPK (Abcam cat#: 23875 RRID:AB_447741), and anti-p-mTOR (Abcam cat#: 109268 RRID:AB_10888105). Then, the sections were washed and incubated with secondary antibodies (Zhongshan Biotech, Beijing, China) at room temperature. The tissue sections were incubated with diaminobenzidine and counterstained

with haematoxylin, dehydrated, and mounted. The sections were viewed under the light microscope.

2.16 | Transmission electron microscopy

Rat hearts were fixed in 2.5% glutaraldehyde overnight and immersed in 1% osmium tetroxide in 0.1-M cacodylate buffer for 1 hr followed by incubation with 2% aqueous uranyl acetate for 2 hr. The samples were dehydrated with a graded series of ethanol and sliced into small grids. Grids were examined with a Philips CM 10 electron microscope operated at 80 kV.

2.17 | Measurement of mitochondrial membrane potential

NRCs were incubated with JC-1 staining solution (Beyotime, Shanghai, China) for 30 min at 37°C. Then, the cells were washed with JC-1 buffer three times. The images were captured by a fluorescence microscope. Red fluorescence represents normal membrane potential, and green fluorescence represents reduced membrane potential. The results were determined by the red/green ratio and analysed by Image J software (RRID:SCR_003070).

2.18 | Data and statistical analysis

The data and statistical analysis comply with the recommendations on experimental design and analysis in pharmacology (Curtis et al., 2018). Randomization was used to assign samples to the experimental groups and treatment conditions for all in vivo studies. Data collection and evaluation of all in vivo and in vitro experiments were performed in a blinded manner. Data was analysed with SPSS 20.0 software (RRID:SCR_002865). All data are expressed as mean \pm SD. Comparisons between multiple groups were evaluated using one-way ANOVA followed by Bonferroni's or Dunnett's T3 tests. Post hoc tests were conducted only if *F* was significant, and there was no variance inhomogeneity. Values of *P* < .05 were considered statistically significant. Data normalization was performed to control for sources of variation of baseline parameters.

2.19 | Nomenclature of targets and ligands

Key protein targets and ligands in this article are hyperlinked to corresponding entries in <http://www.guidetopharmacology.org>, the common portal for data from the IUPHAR/BPS Guide to PHARMACOLOGY (Harding et al., 2018) (RRID:SCR_009017), and are permanently archived in the Concise Guide to PHARMACOLOGY 2017/18 (Alexander, Fabbro et al., 2017; Alexander, Kelly et al., 2017).

3 | RESULTS

3.1 | Spermidine improved cardiomyocyte viability and cardiac dysfunction

To determine the effects of spermidine on cardiomyocyte injury, different concentrations (10, 100, and 1,000 μ M) of spermidine were added to the Ang II-treated cardiomyocytes. The CCK-8 assays showed that 1 μ M of Ang II caused cell death, and the addition of spermidine reversed cardiomyocyte death and significantly enhanced cell viability. The cardiomyocytes treated with 1,000 μ M of spermidine showed the highest level of cell viability (Figure 2a). Thus, 1,000 μ M of spermidine was chosen for the subsequent in vitro experiments. PI staining revealed that spermidine markedly diminished Ang II-induced necrosis in NRCs (Figure 2b). Next, we investigated the role of spermidine in the post-MI rats. Four weeks after MI, the survival analysis demonstrated that 21 of 30 rats survived in the MI group compared to 26 of 30 rats surviving in the MI + SPD group (Figure S1). Additionally, Masson-trichrome staining showed that the infarct size was drastically reduced with SPD treatment in post-MI rats (Figure 2c). Moreover, cardiac function and structure in rats were assessed by echocardiography. Echocardiography analysis revealed that LVEF and LVFS values were significantly lower in MI group than in the sham group, which were improved by spermidine treatment (Figure 2d). Compared to sham group, the LVIDd and LVIDs were critically increased in post-MI rats, but this LV enlargement was decreased by spermidine treatment. However, LV wall thickness which was decreased by MI was not clearly changed by spermidine (Figure S2). In order to further confirm whether spermidine could attenuate MI-induced cardiac hypertrophy, we measured heart to body weight ratio (HW/BW) and found that spermidine significantly reduced HW/BW ratio which was increased in rats with MI (Figure 2e). Furthermore, WGA staining also showed that surface areas of cardiomyocytes were increased in MI group compared to sham group, but spermidine supplement significantly decreased the surface areas which were enlarged by MI (Figure 2f). These data indicated that MI-induced cardiac hypertrophy could be attenuated by spermidine treatment.

3.2 | Spermidine inhibited cardiac oxidative stress, inflammatory reaction, and apoptosis

Previous researches have shown that increased oxidative stress contributed significantly to cardiomyocyte death post-MI (Chen et al., 2016) and we therefore investigated the effects of spermidine on cellular ROS production in NRCs. Exposing NRCs to Ang II markedly increased ROS content, and spermidine significantly inhibited ROS generation (Figure 3a). In post-MI rats, observation in MI + SPD group represented with an elevated level of the anti-oxidase enzyme, SOD, and a reduced level of MDA, compared with the levels in the MI group, revealing that spermidine attenuated myocardial oxidative stress induced by MI (Figure S3). The inflammatory reaction is another

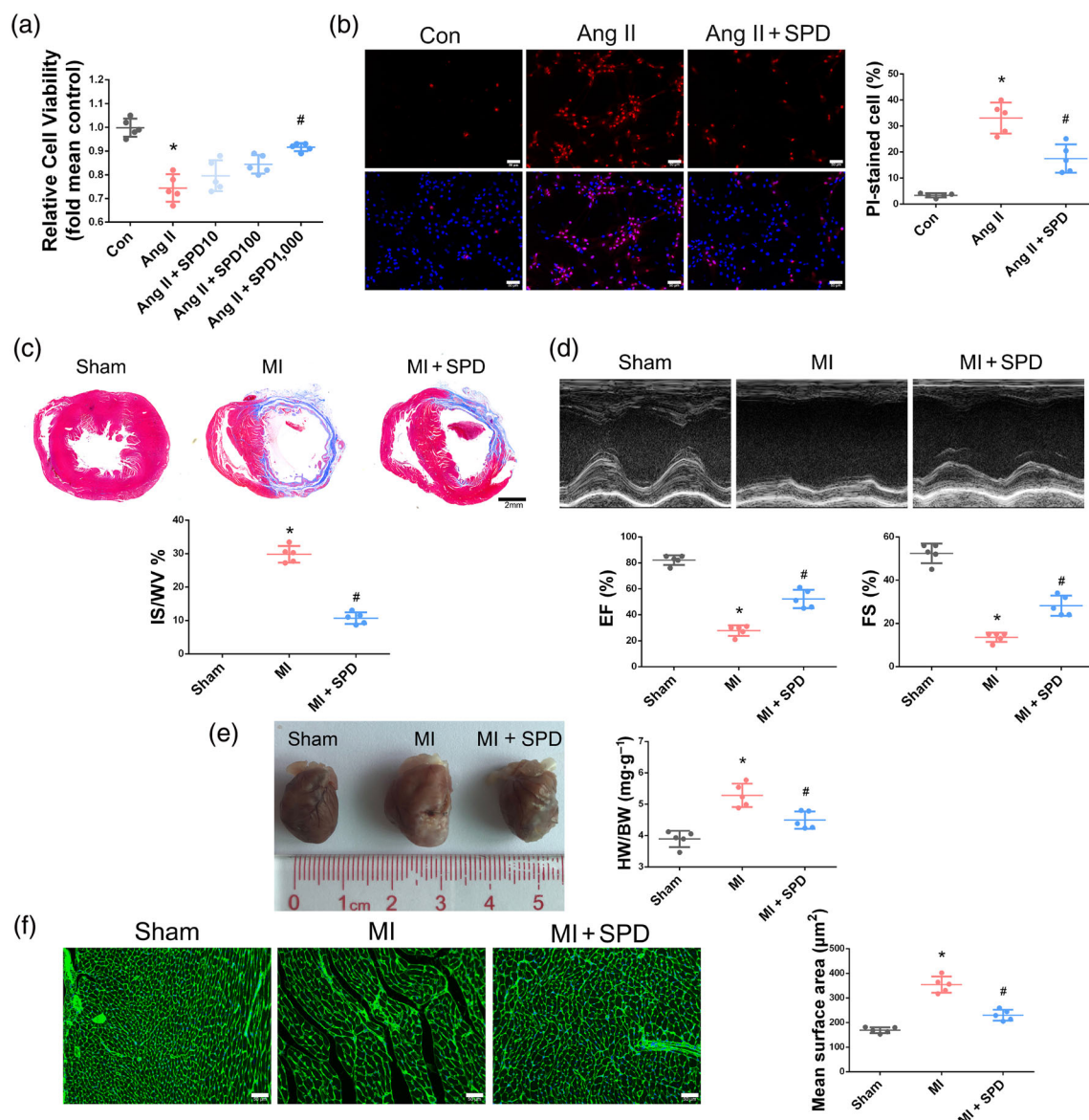


FIGURE 2 Spermidine (SPD) improved cardiomyocyte viability and cardiac dysfunction. (a) Effect of different doses of spermidine on Ang II-treated NRCs was determined. Cell viability was measured by CCK-8 assay. Data shown are individual values with means \pm SD; $n = 5$. * $P < .05$, significantly different from control group, # $P < .05$, significantly different from Ang II group. (b) PI staining was performed to detect necrosis of NRCs. The higher panels indicated that the PI-positive nuclei were stained red. The lower panels indicated that the PI-positive nuclei were merged with total nuclei which were stained with Hoechst 33342. Scale bar represents 50 μ m. Data shown are individual values with means \pm SD; $n = 5$. * $P < .05$, significantly different from control group, # $P < .05$, significantly different from Ang II group. (c) Representative images of myocardial slices with Masson-trichrome staining after MI. Blue staining indicated infarct area. Scale bar represents 2 mm. The graphs show the quantitative analysis. Data shown are individual values with means \pm SD; $n = 5$. * $P < .05$, significantly different from sham group, # $P < .05$, significantly different from MI group. (d) M-mode echocardiography was used to measure left ventricular EF and FS in the different groups. Representative echocardiograms were shown. Summary data shown are individual values with means \pm SD; $n = 5$. * $P < .05$, significantly different from sham group, # $P < .05$, significantly different from MI group. (e) Representative photographs of whole hearts in each group. Ratio of heart weight to body weight ($\text{mg}\cdot\text{g}^{-1}$) is shown. Data shown are individual values with means \pm SD; $n = 5$. * $P < .05$, significantly different from sham group, # $P < .05$, significantly different from MI group. (f) Photomicrographs and quantification of left ventricular tissue sections stained with wheat germ agglutinin (WGA). Scale bar represents 50 μ m. Data shown are individual values with means \pm SD; $n = 5$. * $P < .05$, significantly different from sham group, # $P < .05$, significantly different from MI group

critical component that participates in pathological alteration in the post-MI heart (Francis Stuart, De Jesus, Lindsey, & Ripplinger, 2016; Heusch et al., 2014). The MI + SPD group showed suppressed expression of inflammatory cytokines such as IL-1 β , IL-6, and TNF- α , when

compared with the MI group, suggesting that spermidine could alleviate MI-induced cardiac inflammatory reaction (Figure S4). Furthermore, the effects of spermidine on myocardial apoptosis was assessed both in vivo and in vitro. In vitro, the results of TUNEL

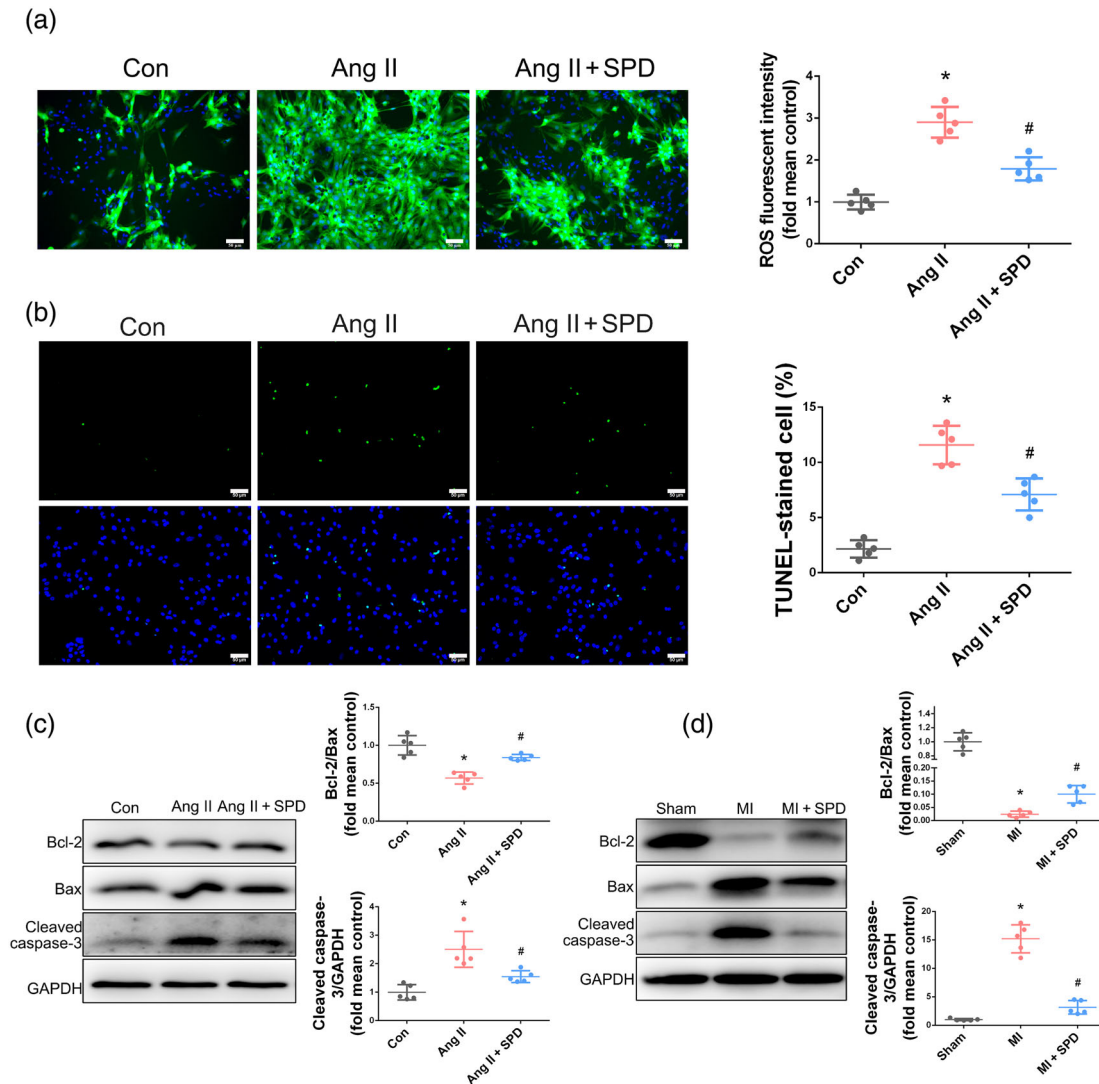


FIGURE 3 Spermidine (SPD) reduced cellular ROS and inhibited myocardial apoptosis. (a) Cellular ROS production stained using DCFH-DA and merged with the total nuclei which were stained with Hoechst 33342. Representative images and quantification of DCFH-DA are shown. Scale bar represents 50 μ m. Data shown are individual values with means \pm SD; $n = 5$. * $P < .05$, significantly different from control group, # $P < .05$, significantly different from Ang II group. (b) Representative photomicrographs and quantification of TUNEL staining in NRCs. The higher panels indicated that the TUNEL-positive nuclei were stained green. The lower panels indicated that the TUNEL-positive nuclei were merged with total nuclei which were stained with DAPI. Scale bar represents 50 μ m. Data shown are individual values with means \pm SD; $n = 5$. * $P < .05$, significantly different from control group, # $P < .05$, significantly different from Ang II group. (c) Western blot of cleaved caspase-3, Bcl-2, and Bax in Ang II-treated NRCs. Data shown are individual values with means \pm SD; $n = 5$. * $P < .05$, significantly different from control group, # $P < .05$, significantly different from Ang II group. (d) Western blot of cleaved caspase-3, Bcl-2, and Bax in post-MI rats. The quantification of cleaved caspase-3/GAPDH and Bcl-2/Bax is shown. Data shown are individual values with means \pm SD; $n = 5$. * $P < .05$, significantly different from sham group, # $P < .05$, significantly different from MI group

staining showed that spermidine inhibited the apoptosis of Ang II-treated NRCs (Figure 3b). Moreover, the protein expression of cleaved caspase-3, a marker of apoptosis, was down-regulated, and the ratio of Bcl-2/Bax was increased in the presence of spermidine, compared with NRCs exposed to Ang II treatment alone (Figure 3c). In vivo, these effects were still present as protein expression of cleaved caspase-3 and Bcl-2/Bax ratio in the MI + SPD group were changed in accordance with in vitro findings, when compared to MI group (Figure 3d). It was clear that spermidine could inhibit oxidative stress and cardiac inflammation and reduce myocardial apoptosis in post-MI rats.

3.3 | Spermidine restored autophagic flux in Ang II-treated NRCs

Recent studies have proposed that spermidine can induce autophagy in several cellular models (Yang et al., 2017; Zheng et al., 2018). Thus, to determine whether stimulation with spermidine might promote autophagic flux in Ang II-treated NRCs, protein expression of the autophagy-associated molecules (LC3 II and p62) was evaluated after spermidine administration. Levels of LC3 II and p62 were elevated in Ang II-treated NRCs and the accumulation of these proteins indicated

that the autophagic flux might be interrupted. Addition of spermidine to Ang II-treated NRCs reduced the levels of LC3 II and p62, indicating a restoration of autophagic flux (Figure 4a,b). To further confirm the role of spermidine in the modulation of autophagic flux, CQ (an autophagy inhibitor) was used to block autophagosome turnover. Both Ang II + SPD + CQ group and Ang II + CQ group displayed a markedly increased expression of LC3 II and p62, suggesting that CQ inhibited autophagosome degradation, a process that spermidine failed to modify (Figure 4c,d).

Also, the tandem fluorescence mRFP-GFP-LC3 analysis was performed on NRCs to test the capacity of spermidine to enhance autophagic flux. Ad-LC3-NRCs incubated with Ang II displayed an accumulation of autophagosomes and a few autolysosomes, with a markedly elevated autophagosome/autolysosome ratio, suggesting that autophagosome clearance was inhibited and autophagic flux was blocked. Treatment of these cells with spermidine led to large amounts of autolysosomes and a few autophagosomes, with a decreased level of autophagosomes/autolysosomes ratio, indicating

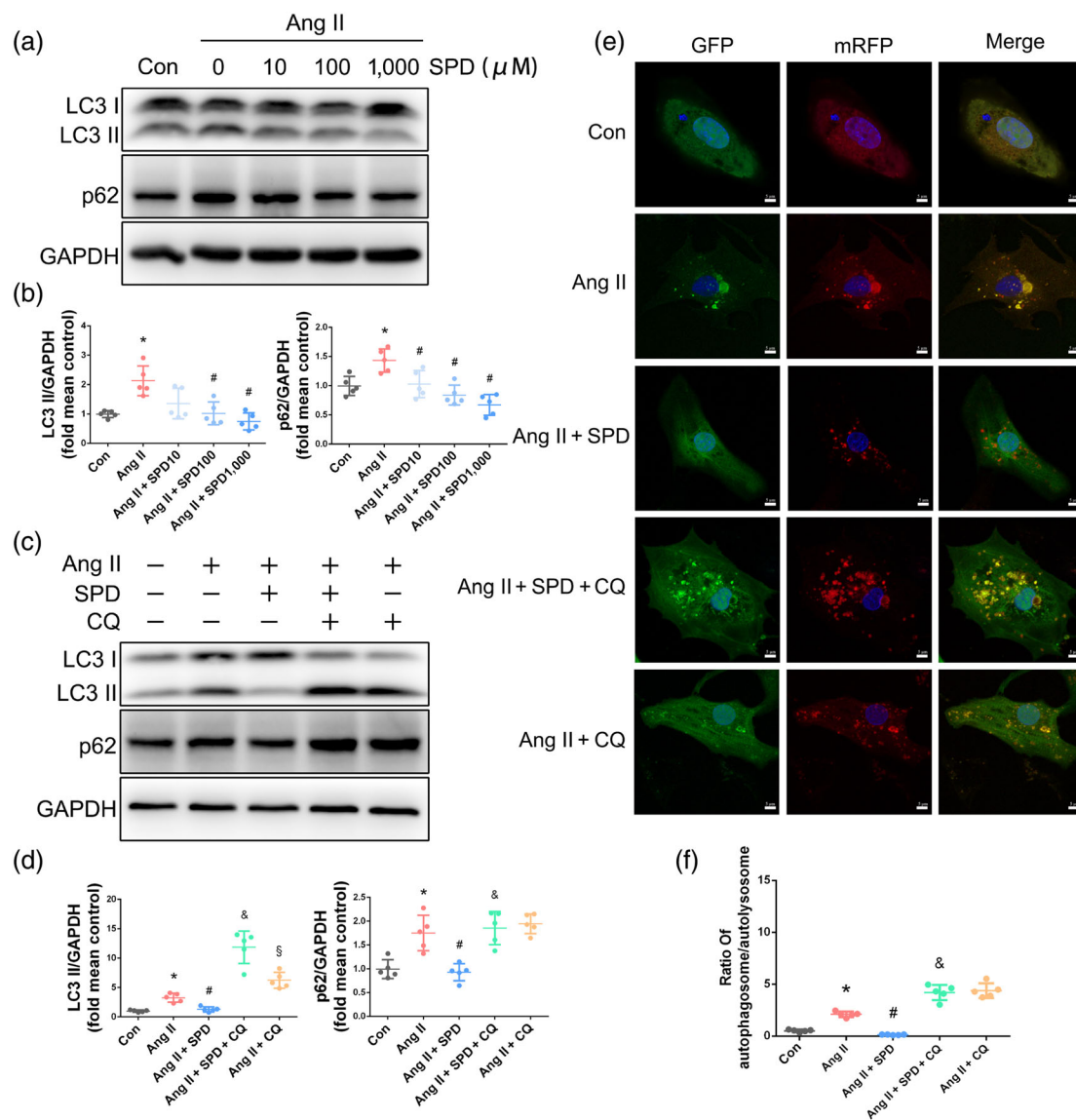


FIGURE 4 Spermidine (SPD) restored autophagic flux in Ang II-treated NRCs. (a) Expression of LC3 II and p62 in NRCs treated with Ang II and 10-, 100-, and 1,000- μ M SPD. (b) Quantitative analysis of panel (a). Data shown are individual values with means \pm SD; $n = 5$. * $P < .05$, significantly different from control group, # $P < .05$, significantly different from Ang II group. (c) Representative western blots of LC3 II and p62 in different groups. (d) Quantification for panel (c). Data shown are individual values with means \pm SD. $n = 5$, * $P < .05$, significantly different from control group, # $P < .05$, significantly different from Ang II group, & $P < .05$, significantly different from Ang II + SPD group, & $P < .05$, significantly different from Ang II + SPD + CQ group. (e) NRCs transfected with adenovirus harbouring tandem fluorescent mRFP-GFP-LC3 were exposed to different treatments for monitoring autophagic flux. Representative images of immunofluorescent NRCs expressing mRFP-GFP-LC3 were shown. The nuclei stained with DAPI are blue; GFP dots were green; mRFP dots were red. Scale bar represents 5 μ m. (f) The autophagosomes/autolysosomes ratio was presented and quantitatively analysed. Data shown are individual values with means \pm SD. * $P < .05$, significantly different from control group, # $P < .05$, significantly different from Ang II group, & $P < .05$, significantly different from Ang II + SPD group

that spermidine increased autophagic flux and promoted degradation of excessive autophagosomes. However, after co-treatment with CQ, the effect of spermidine on enhancing autophagic flux was blocked, as reflected by the up-regulation of autophagosomes/autolysosomes ratio in the Ang II + SPD + CQ group compared with that in the Ang II + SPD group (Figure 4e,f).

3.4 | Spermidine enhanced autophagic flux in post-MI rats

In a recent study, spermidine-induced autophagic flux exerted cardioprotective effects on aging- and hypertension-related cardiac dysfunction (Eisenberg et al., 2016). To test whether spermidine enhances autophagic flux in post-MI rats, the expression of LC3 II and p62 was measured. LC3 II expression was up-regulated, and p62 expression was decreased markedly in the MI + SPD group, compared with that in the MI group, suggesting that spermidine potentially

enhanced autophagic flux in post-MI rats. After CQ treatment, the expression of LC3 II and p62 was significantly increased, confirming that autophagosome turnover was blocked by CQ treatment. There were no significant differences of LC3 II and p62 expression between MI + SPD + CQ group and MI + CQ group (Figure 5a,b). Consistent with the western blot data, immunohistochemistry analysis also showed that spermidine increased LC3 B expression and decreased p62 expression in post-MI rats (Figure 5c).

3.5 | Spermidine-enhanced autophagic flux decreased myocardial apoptosis in vitro and in vivo

In vitro TUNEL assays revealed that spermidine treatment could significantly reduce the apoptosis of NRCs exposed to Ang II. However, the anti-apoptotic effect of spermidine was abolished by the autophagy inhibitor CQ, suggesting that the enhancement of autophagic flux is required for the anti-apoptotic effect of spermidine

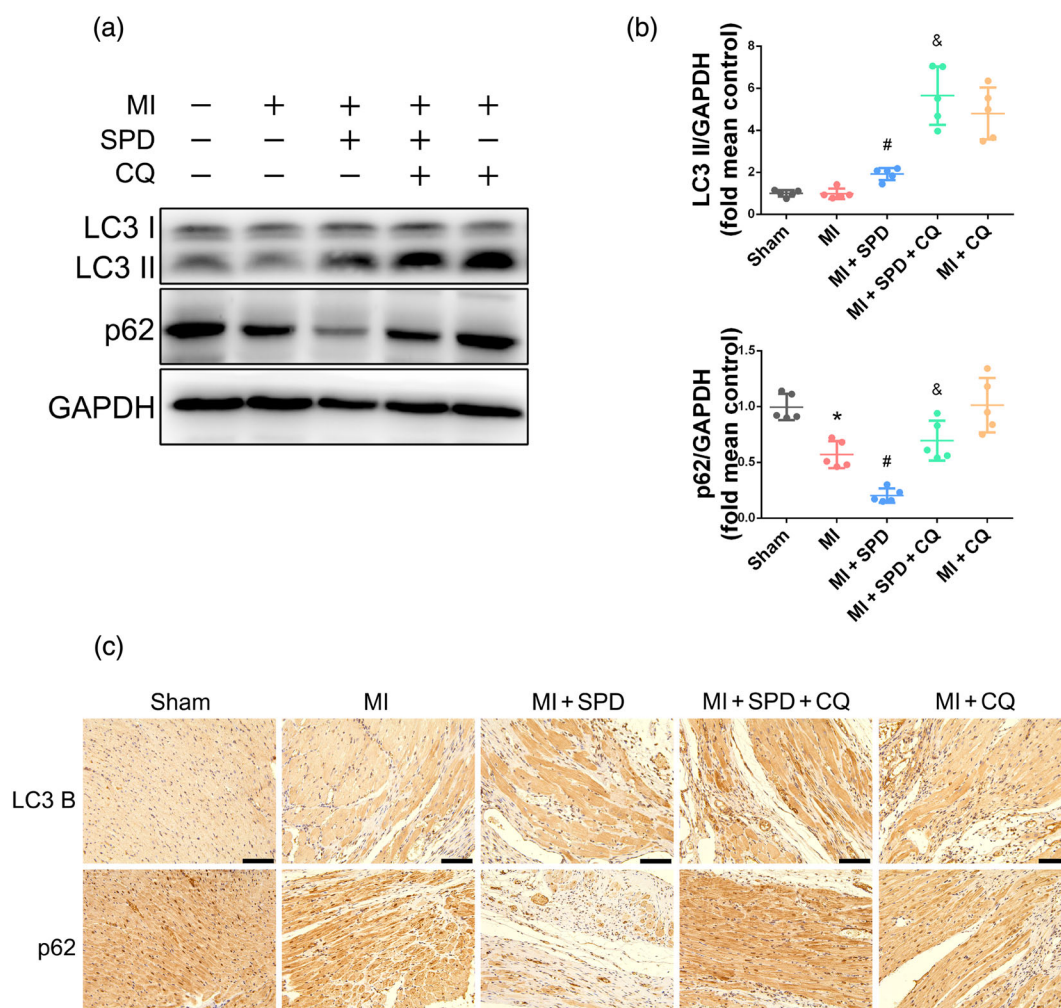


FIGURE 5 Spermidine (SPD) enhanced autophagic flux in post-MI rats. (a) Western blotting analysis of LC3 B and p62 in rats with different treatments. (b) Semi-quantification for panel (a). Data shown are individual values with means \pm SD; $n = 5$. * $P < .05$, significantly different from sham group, # $P < .05$, significantly different from MI group, & $P < .05$, significantly different from MI + SPD group. (c) Immunostaining of the LC3 B and p62 in post-MI rats with different treatments. Scale bar represents 100 μ m

(Figure 6a). Similarly, in vivo TUNEL analysis showed that apoptosis increased in infarcted hearts, compared with those from sham group, and spermidine supplementation reduced myocardial apoptosis, but this effect could be blocked by CQ treatment (Figure 6b). Also, the

anti-apoptotic effects of spermidine were shown in the western blots, as indicated by down-regulation of cleaved caspase-3 and up-regulation of the Bcl-2/Bax ratio, but these effects were abolished after treatment with CQ, in vitro and in vivo (Figure 6c,d).

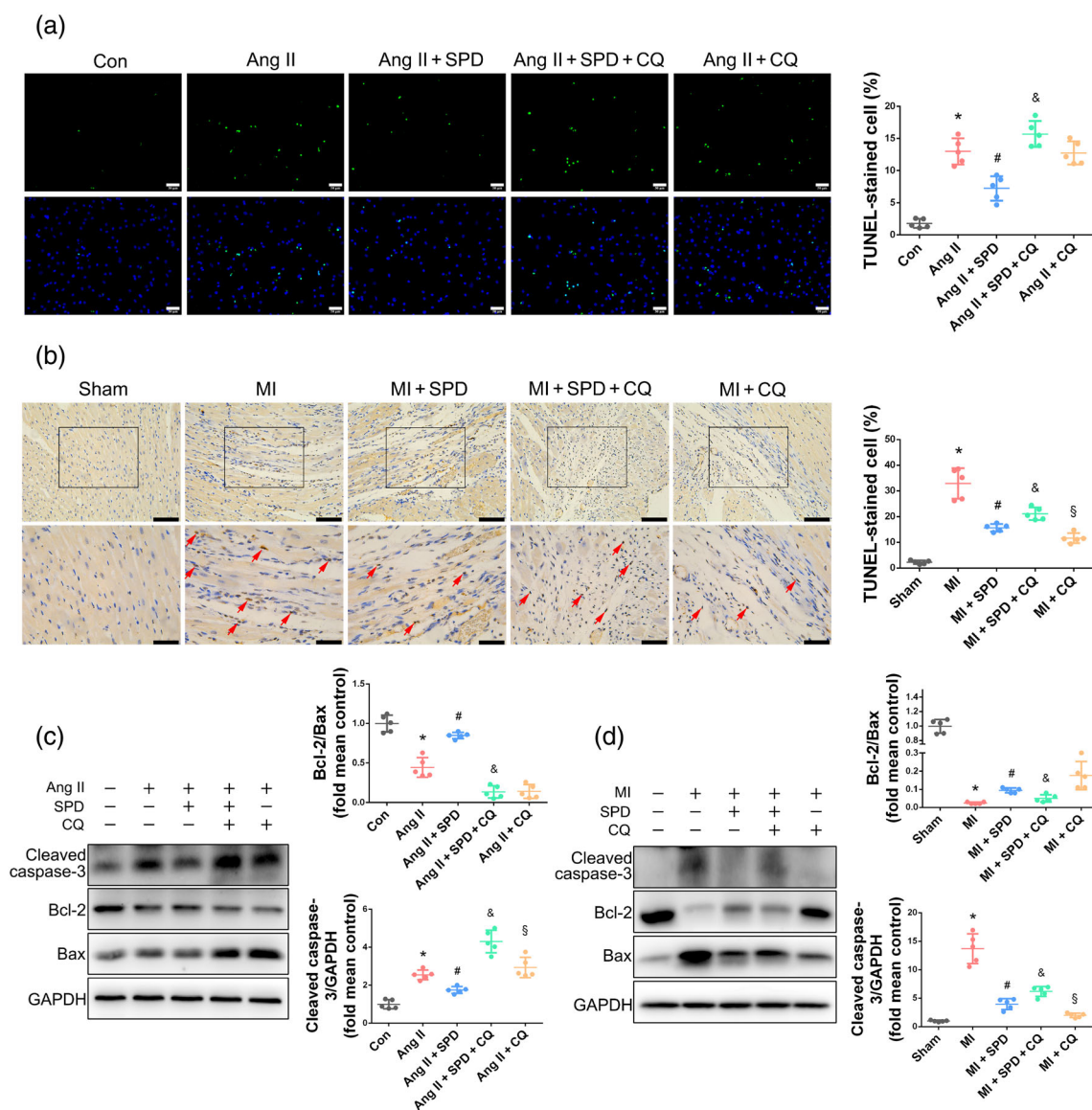


FIGURE 6 Spermidine (SPD) decreased myocardial apoptosis depending on enhancing autophagic flux. (a) Representative images and quantification of TUNEL staining in NRCs with different treatments. Green dots were regarded as TUNEL-positive cells. Blue dots were total nuclei which were stained with DAPI. Scale bar represents 50 μ m. Data shown are individual values with means \pm SD; $n = 5$. * $P < .05$, significantly different from control group, # $P < .05$, significantly different from Ang II group, & $P < .05$, significantly different from Ang II + SPD group. (b) Apoptotic cardiomyocytes were detected using TUNEL staining. Cardiomyocytes with brown nuclei were interpreted as TUNEL-positive cells, and total nuclei were stained blue with DAPI. The representative photos and quantitative analysis were presented. Scale bar represents 100 μ m. Data shown are individual values with means \pm SD; $n = 5$. * $P < .05$, significantly different from sham group, # $P < .05$, significantly different from MI group, & $P < .05$, significantly different from MI + SPD group, & $P < .05$, significantly different from MI + SPD + CQ group. (c) Representative western blotting pictures and quantitative analysis of cleaved caspase-3, Bcl-2, and Bax in Ang II-treated NRCs with different treatments. Data shown are individual values with means \pm SD; $n = 5$. * $P < .05$, significantly different from control group, # $P < .05$, significantly different from Ang II group, & $P < .05$, significantly different from Ang II + SPD group, & $P < .05$, significantly different from Ang II + SPD + CQ group. (d) Representative western blotting pictures and quantitative analysis of cleaved caspase-3, Bcl-2, and Bax in post-MI rats with different treatments. Data shown are individual values with means \pm SD; $n = 5$. * $P < .05$, significantly different from sham group, # $P < .05$, significantly different from MI group, & $P < .05$, significantly different from MI + SPD group, & $P < .05$, significantly different from MI + SPD + CQ group

3.6 | Spermidine-enhanced autophagic flux improved cardiac dysfunction and attenuated myocardial injury

Previous studies have revealed that the longevity-promoting and neuroprotective effects of spermidine were abolished after knockout of autophagy-related genes (Eisenberg et al., 2009; Gupta et al., 2013). Here, we have investigated whether spermidine exerted

cardioprotective effects by enhancing autophagic flux. The Masson-trichrome staining showed that spermidine clearly reduced infarct size induced by MI, but this effect was partly eliminated by CQ co-treatment (Figure 7a). M-mode echocardiography revealed that LVFS and LVEF values were improved by spermidine, but this effect was partly blocked after CQ co-treatment, suggesting the involvement of autophagic flux in spermidine induced improvement of cardiac function (Figure 7b). We also performed echocardiography to evaluate

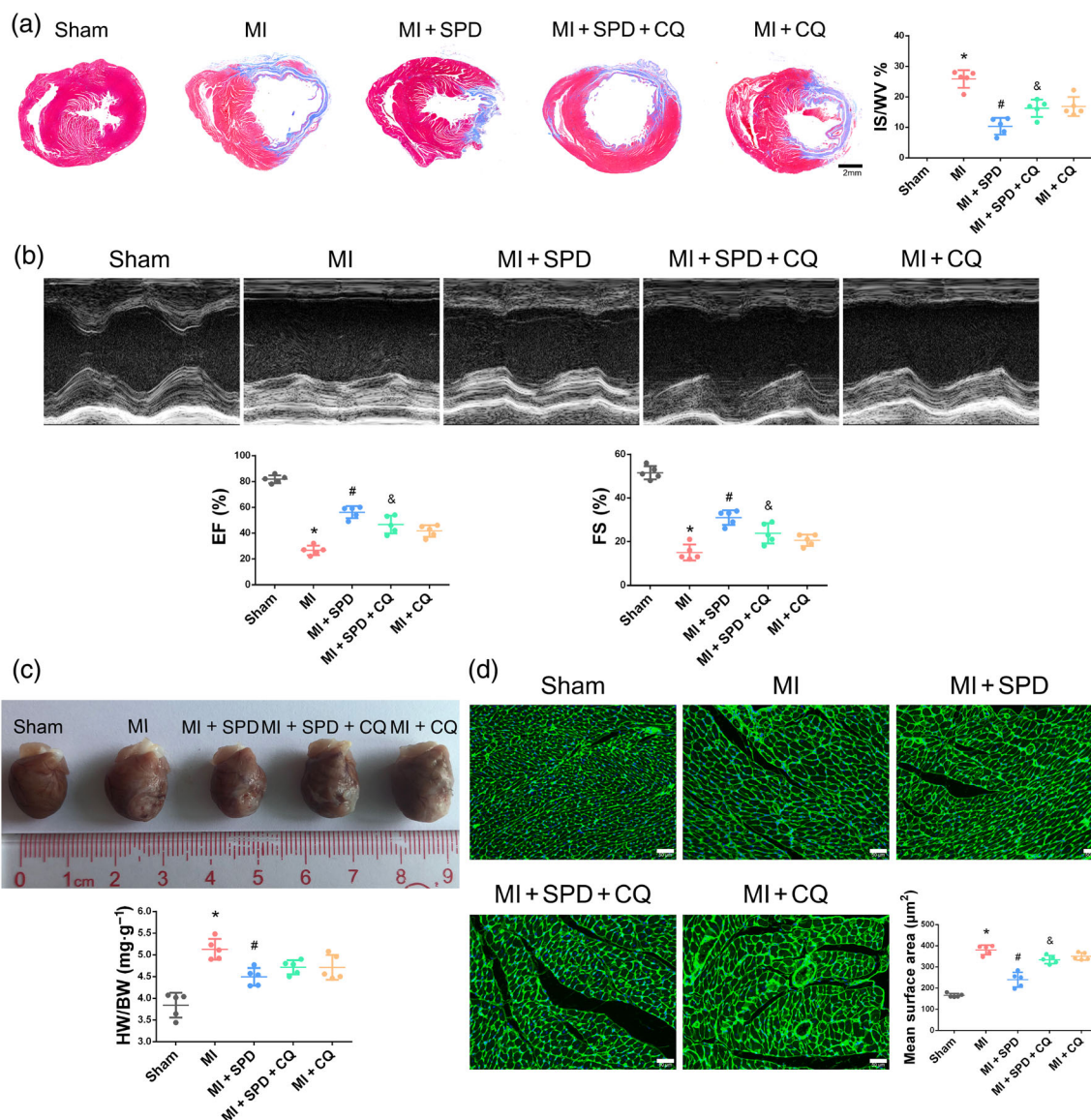


FIGURE 7 Spermidine (SPD) attenuated cardiac dysfunction partially through enhancing autophagic flux. (a) Representative images of Masson-trichrome staining in different groups. Myocardial fibrosis was stained blue representing myocardial infarct size. The infarct size/whole ventricle ratio is shown. Scale bar represents 2 mm. Data shown are individual values with means \pm SD; $n = 5$. * $P < .05$, significantly different from sham group, $^{\#}P < .05$, significantly different from MI group, $^{\&}P < .05$, significantly different from MI + SPD group. (b) Representative echocardiograms and measurements from rats with different treatments. LVEF and LVFS were measured and calculated. Data shown are individual values with means \pm SD; $n = 5$. * $P < .05$, significantly different from sham group, $^{\#}P < .05$, significantly different from versus MI group, $^{\&}P < .05$, significantly different from MI + SPD group. (c) Representative photographs of whole hearts from each group. Ratio of heart weight to body weight ($\text{mg}\cdot\text{g}^{-1}$) is shown. Data shown are individual values with means \pm SD. $n=5$, * $P < .05$, significantly different from sham group, $^{\#}P < .05$, significantly different from MI group. (d) Representative photomicrographs and quantitative analysis of left ventricular tissue sections stained with wheat germ agglutinin (WGA). Scale bar represents 50 μm . Data shown are individual values with means \pm SD; $n = 5$. * $P < .05$, significantly different from sham group, $^{\#}P < .05$ versus MI group, $^{\&}P < .05$ versus MI + SPD group

the role of autophagic flux in spermidine-improved cardiac hypertrophy and found that CQ could not markedly weaken spermidine-improved LVIDd and LVIDs (Figure S5). Moreover, HW/BW ratio was decreased by spermidine supplementation and CQ also could not significantly inhibit this effect (Figure 7c). Additionally, WGA staining showed that the surface area of cardiomyocytes was decreased by spermidine treatment, but that this effect was partly abated by CQ co-treatment (Figure 7d). Next, the role of spermidine on myocardial cell composition was investigated by transmission electron microscopy. Abundant tight mitochondria, neatly arranged, and intact myofibrils

could be seen in the cytoplasm of myocardial cells from the sham group. In contrast, MI group had fewer mitochondria and more ruptured myofibrils, compared with those in the sham group. However, MI-induced reduction of mitochondrial and myofibrillar areas was reversed by spermidine treatment, and this effect was partly blocked by CQ co-treatment (Figure 8a,b). Furthermore, in vitro JC-1 staining showed that spermidine reversed the mitochondrial membrane potential reduction induced by Ang II but that this effect was blunted by CQ, indicating that spermidine prevented the decrease in mitochondrial membrane potential, by enhancing autophagic flux (Figure 8c,d). These

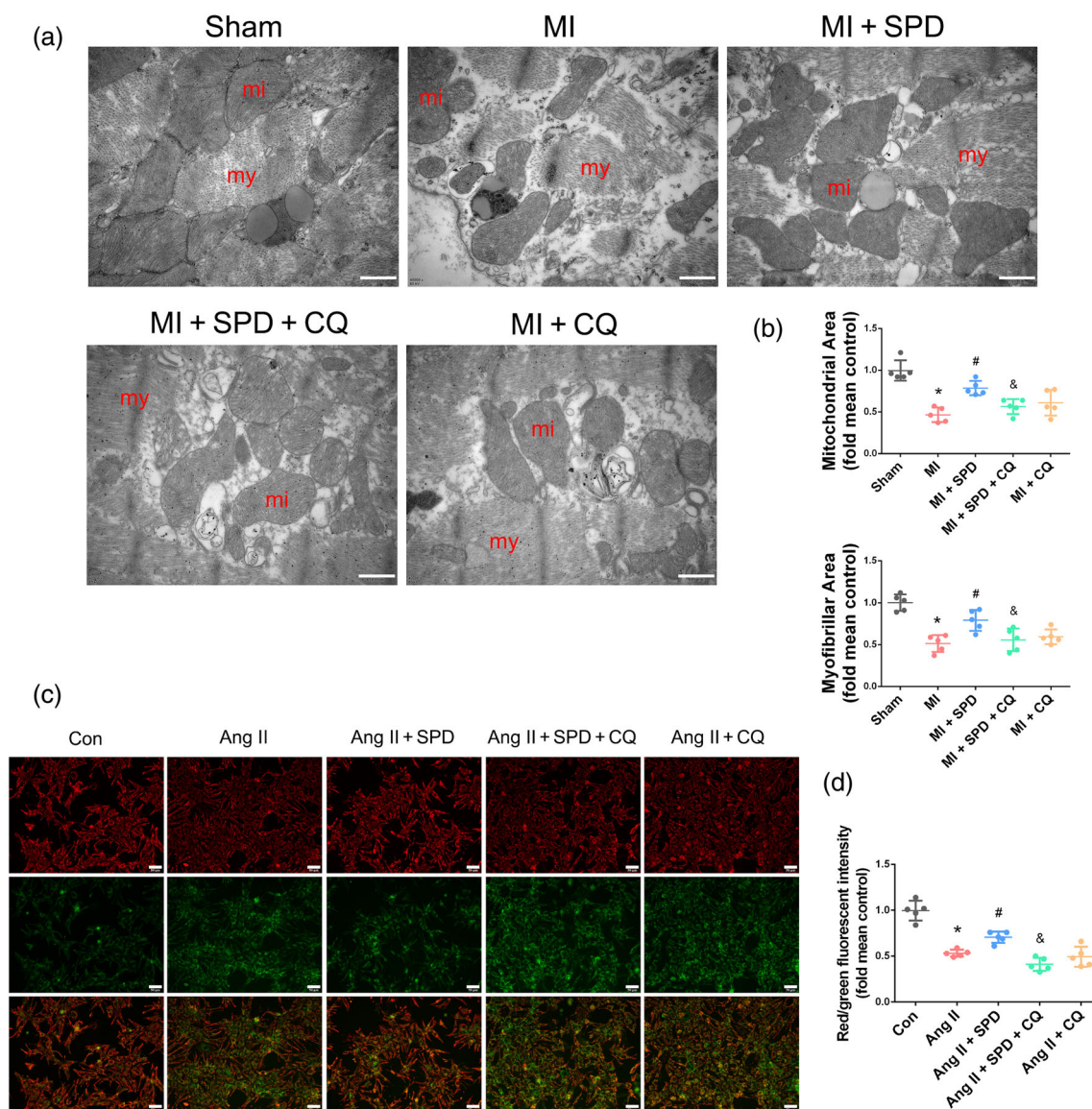


FIGURE 8 Spermidine (SPD) alleviated myocardial injury, partly by increasing autophagic flux. (a) Representative images, obtained by TEM, of cardiomyocyte mitochondria and myofibril in different groups. Mitochondria (Mi) and Myofibril (My) were marked in red. Scale bar represents 500 nm. (b) Quantification of panel (a). Data shown are individual values with means \pm SD. * $P < .05$, significantly different from sham group, # $P < .05$, significantly different from MI group, & $P < .05$, significantly different from MI + SPD group. (c) Mitochondrial membrane potential was estimated with JC-1 staining and captured by the microscope. Red fluorescence represented intact mitochondrial membrane potential. Green fluorescence represented reduced mitochondrial membrane potential. Scale bar represents 50 μ m. (d) Quantification of panel (c). Data shown are individual values with means \pm SD; $n = 5$. * $P < .05$, significantly different from control group, # $P < .05$, significantly different from Ang II group, & $P < .05$, significantly different from Ang II + SPD group

data showed that spermidine attenuated MI-related cardiac dysfunction and myocardial injury at least partly through promotion of autophagic flux.

3.7 | Spermidine promoted autophagic flux via the AMPK/mTOR pathway in vitro and in vivo

Previous studies have shown that the AMPK/mTOR signalling pathway plays a crucial role in the activation of autophagic flux (L. Sun et al., 2015; Zhong et al., 2017). We therefore tested the involvement of the AMPK/mTOR signalling pathway in autophagic flux activation by spermidine. We used the AMPK-specific inhibitor Compound C to investigate whether AMPK/mTOR signalling was essential for spermidine-induced autophagic flux in our study. Spermidine treatment significantly increased the phosphorylation of AMPK (p-AMPK) and reduced the phosphorylation of mTOR (p-mTOR) both in vitro and in vivo. After treatment with Compound C, the levels of p-AMPK and p-mTOR were restored and the effect of spermidine on modulating LC3 II and p62 was lost, both in vitro and in vivo, demonstrating that the activation of autophagic flux was abolished, following inhibition of AMPK by Compound C (Figure 9a–d). Immunohistochemical staining for the AMPK/mTOR signal showed similar results and together demonstrated that spermidine enhanced autophagic flux through the AMPK/mTOR signalling pathway (Figure 9e).

4 | DISCUSSION

This study suggested for the first time that spermidine exerts cardioprotective effects against MI through enhancing autophagic flux. Our study indicated that (a) spermidine ameliorates MI-induced myocardial injury and cardiac dysfunction; (b) spermidine exerts cardioprotective effects at least partially depending on enhancing autophagic flux following MI; and (c) spermidine promotes autophagic flux through AMPK/mTOR signalling pathway after MI. The significant findings in this study were illustrated in Figure 10.

A recent study has reported that spermidine intake correlates inversely with the incidence and mortality of cardiovascular disease in the Bruneck cohort (Eisenberg et al., 2016). In our study, we found that spermidine alleviated myocardial injury and cardiac dysfunction against MI in rats, which might provide evidence to explain why spermidine can reduce the risk of cardiovascular diseases. However, it is still controversial of the association between spermidine level and development of cardiovascular disease. Sansbury et al. found that polyamine metabolites including putrescine and SPD were increased after transverse aortic constriction or MI surgery in mice and negatively correlated with LVEF (Sansbury et al., 2014). In contrast, it was proposed that spermidine content positively correlated with the LVEF in patients with heart failure (Meana et al., 2016). This discrepancy might be explained by different experimental subjects and conditions. However, our study showed that exogenous spermidine supplement could significantly improve LVEF and LVFS and limit

infarct size in post-MI rats. Eisenberg et al. suggested that spermidine supplementation improves cardiac function, reduces ventricular hypertrophy, and delays the progression of heart failure in rats with salt-induced hypertension (Eisenberg et al., 2016). In agreement with this study, we found that spermidine significantly improved cardiac function and reversed cardiac hypertrophy in post-MI rats. However, whether spermidine attenuate myocardial hypertrophy and ventricular remodelling depending on autophagic flux is not fully understood and deserves in-depth investigation.

Autophagy is a catabolic pathway participating in the breakdown of long-lived proteins and removing excess or dysfunctional cytoplasmic components and organelles (Galluzzi, Pietrocola, Levine, & Kroemer, 2014). Autophagic flux is a dynamic and multistep process that involves the formation of autophagosomes, the fusion of autophagosomes with lysosomes, and the degradation of the autophagosomes. Our previous studies suggested that induction of autophagy attenuates myocardial ischaemia and reperfusion injury (Fu et al., 2018; Ling et al., 2016; Zhong et al., 2017). On the contrary, some studies suggested that excessive autophagy can aggravate cardiac ischaemia–reperfusion injury (Ma et al., 2012). Interestingly, it has also been reported that up-regulating autophagy at a moderate level contributes to cell survival (Tannous et al., 2008), whereas excessive activation of autophagy leads to cell death (Kroemer & Levine, 2008). Similarly, in our study, we found that spermidine reduces apoptosis by enhancing autophagic flux in Ang II-treated NRCs. However, after co-treatment with CQ, spermidine induced an abundance of autophagosomes and led to more apoptosis. These paradoxical findings might be interpreted by the level of the autophagic flux. Moderate increase of autophagy can enhance the autophagic flux, a process that is required for maintaining cell survival. On the contrary, excessive increase of autophagy blocks the autophagic flux and leads to cell death. In this study, we speculated that a moderate autophagosomes/autolysosomes ratio representing intact autophagosome turnover contribute to cell survival and function. A high autophagosomes/autolysosomes ratio could represent impaired autophagosome clearance and might account for excessive apoptosis. Based on our findings, we hypothesized that enhancing autophagic flux instead of merely inducing autophagosome formation, is beneficial for myocardial survival.

After MI, both oxidative stress and inflammatory responses have been reported to cause myocardial injury (Nian, Lee, Khaper, & Liu, 2004; Hori & Nishida, 2009), and suppression of oxidative damage and inflammation successfully attenuates cardiac dysfunction following MI (Hu et al., 2018). In this study, we found that spermidine significantly inhibited oxidative stress and reduced the levels of the inflammatory cytokines following MI. Previous studies have shown spermidine gain its antioxidative and anti-inflammatory effects in association with autophagy induction (LaRocca, Gioscia-Ryan, Hearon, & Seals, 2013; Madeo et al., 2018). In our study, the antioxidative and anti-inflammatory effects of spermidine might also be related to autophagic flux. Furthermore, a previous study revealed that spermidine increased production of NO results in vasodilation, vascular regeneration, and prevention of cardiac remodelling (Knott

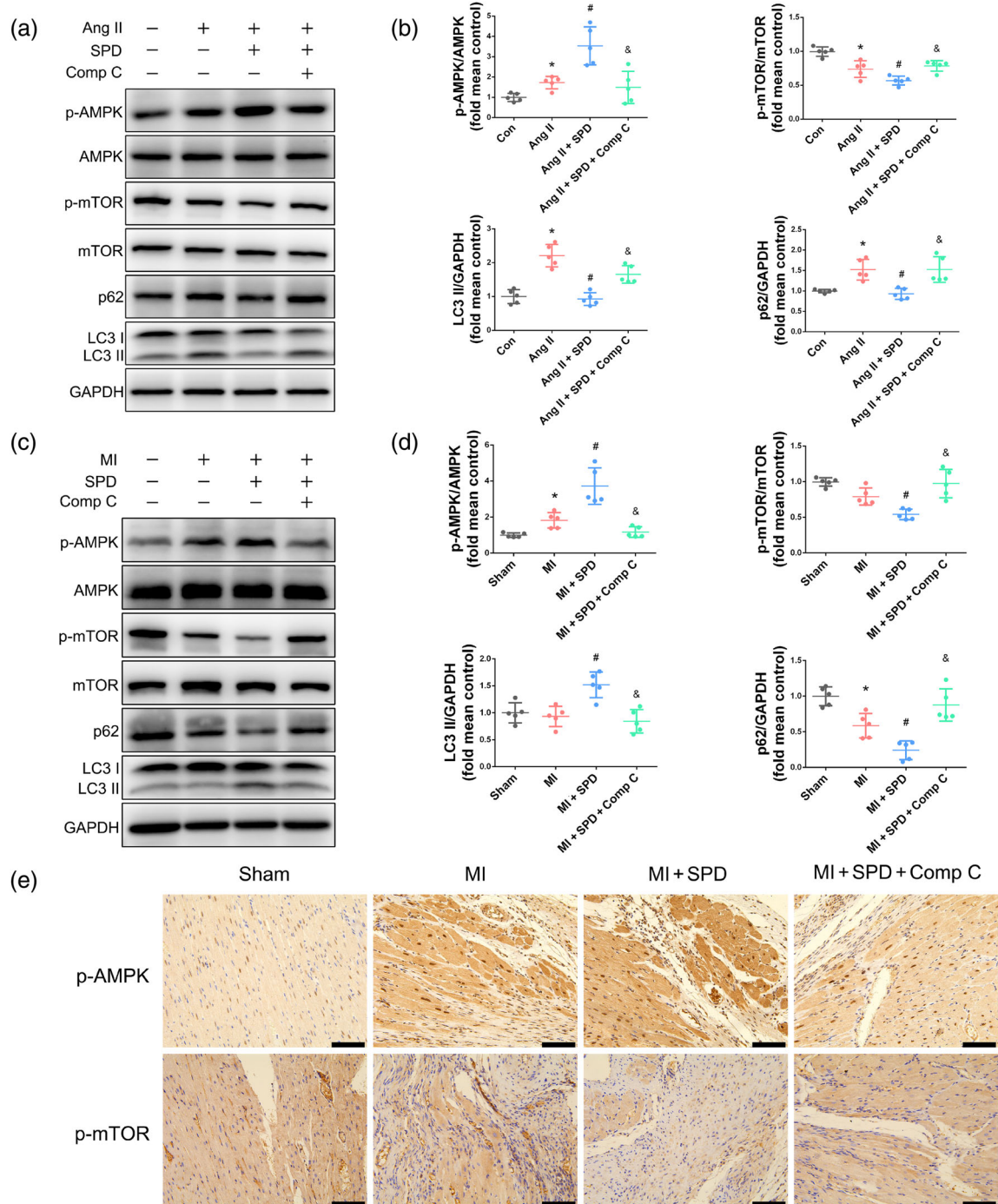


FIGURE 9 Spermidine (SPD) promoted autophagic flux via activation of the AMPK-mTOR pathway in vitro and in vivo. (a) Representative western blots of p-AMPK, AMPK, p-mTOR, mTOR, LC3 II, and p62 in each group in vitro. (b) The levels of p-AMPK/AMPK, p-mTOR/mTOR, LC3 II/GAPDH, and p62/GAPDH were quantified. Data shown are individual values with means ± SD; $n = 5$. * $P < .05$, significantly different from control group, # $P < .05$, significantly different from Ang II group, & $P < .05$, significantly different from Ang II + SPD group. (c) Western blotting analysis of p-AMPK, AMPK, p-mTOR, mTOR, LC3 II, and p62 in different groups in vivo. (d) Semi-quantification for panel (c). Data shown are individual values with means ± SD; $n = 5$. * $P < .05$, significantly different from sham group, # $P < .05$, significantly different from MI group, & $P < .05$, significantly different from MI + SPD group. (e) IHC staining for p-AMPK and p-mTOR. Scale bar represents 100 μm

& Bossy-Wetzel, 2010). Similarly, we found that spermidine supplementation increased NO content in the cardiac tissues after MI (data not shown). It seems plausible that the SPD-induced NO was associated with improvement of the cardiac dysfunction that occurred in the post-MI rats. It has been noted in preceding study that SPD-

induced autophagy is capable of preventing muscle stem cell senescence and improving muscle regeneration in aging mice (García-Prat et al., 2016); however, whether spermidine can induce putative cardiac stem cell for cardiomyocytes regeneration after MI needs further careful research.

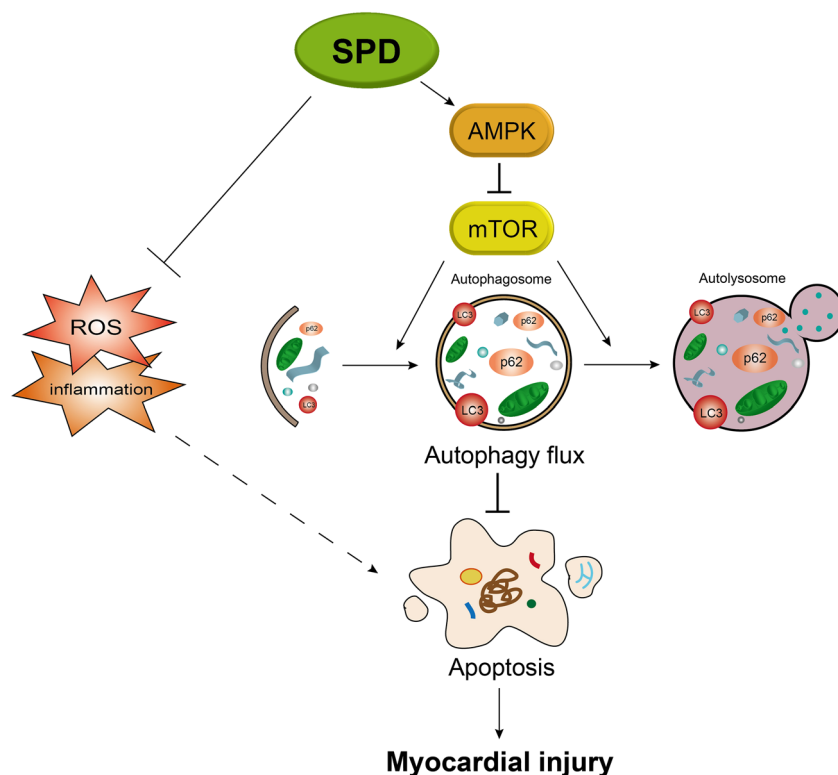


FIGURE 10 Spermidine (SPD) stimulated the AMPK/mTOR pathway in order to enhance autophagic flux and thus alleviated myocardial injury after MI. Additionally, suppression of oxidative stress and inflammatory responses by spermidine could also contribute to the amelioration of MI-induced myocardial injury

AMPK signalling plays a major role in various physiological and pathological cellular events that occur in cardiovascular diseases (Daskalopoulos, Dufeys, Beauloye, Bertrand, & Horman, 2016). AMPK is one of the master checkpoints of cellular metabolism and promotes autophagy by inhibiting mTOR (Ha & Kim, 2016). Our previous study showed that AMPK/mTOR-mediated autophagy exerts protective effects against myocardial damage in diabetic rats (Zhang et al., 2017). In our study, we found that spermidine enhanced autophagic flux by stimulation of AMPK/mTOR signalling pathway in Ang II-treated NRCs and post-MI rats. However, after co-treatment with Compound C, the effect of spermidine on autophagic flux was abolished. It is possible that spermidine reduces myocardial injury and dysfunction following MI at least partially by activation of AMPK/mTOR signalling pathway. Some studies have shown that AMPK stimulation is beneficial during cardiac hypertrophy (Hernández, Barreto-Torres, Kuznetsov, Khuchua, & Javadov, 2014), ventricular remodelling (Noppe et al., 2014), and heart failure (Beauloye, Bertrand, Horman, & Hue, 2011). Taken together, we speculated that AMPK is a positive regulator in SPD-induced cardio-protective effect against MI and that AMPK-mediated protective effects occur at least partially through stimulation of autophagic flux. Nevertheless, the precise mechanisms for SPD-activated AMPK signalling in post-MI rats have not yet to be entirely investigated and demands future exploration.

In conclusion, our study demonstrated that spermidine attenuates myocardial injury and cardiac dysfunction following MI by promoting autophagic flux via activation of AMPK/mTOR pathway. Pharmacological or nutritional intervention with spermidine may become a promising modality for the prevention or treatment of MI.

ACKNOWLEDGEMENTS

This work was supported by the National Natural Science Foundation of China (81400190, 81470488, and 81873460) and the Natural Science Foundation of Guangdong Province (2015A030310478 and 2017A030313703).

CONFLICT OF INTEREST

The authors declare no conflicts of interest.

AUTHOR CONTRIBUTIONS

C.A.H. guided the project. C.A.H., W.X.B., Y.P.Z., and Y.J. conceived and designed the experiments. Y.J., W.Y.X., W.S.Y., and L.H.Q. performed the experiments. L.Y.N., S.X.D., L.Q.C., and Z.Y. analysed the data. Y.J. and Y.J.Y. primarily wrote the manuscript. Y.J.Y., L.Y.N., and W.Y.X. provided revision of the paper. All authors read and approved the manuscript.

DECLARATION OF TRANSPARENCY AND SCIENTIFIC RIGOUR

This Declaration acknowledges that this paper adheres to the principles for transparent reporting and scientific rigour of preclinical research as stated in the *BJP* guidelines for [Design & Analysis](#), [Immunoblotting and Immunocytochemistry](#), and [Animal Experimentation](#), and as recommended by funding agencies, publishers and other organisations engaged with supporting research.

ORCID

Jian-Yun Yan  <https://orcid.org/0000-0002-6962-1169>

Ai-Hua Chen  <https://orcid.org/0000-0001-9395-7052>

REFERENCES

- Alexander, S. P. H., Fabbro, D., Kelly, E., Marrion, N. V., Peters, J. A., Faccenda, E., ... CGTP Collaborators. (2017). The Concise Guide to PHARMACOLOGY 2017/18: Enzymes. *British Journal of Pharmacology*, 174, S272–S359. <https://doi.org/10.1111/bph.13877>
- Alexander, S. P. H., Kelly, E., Marrion, N. V., Peters, J. A., Faccenda, E., Harding, S. D., ... CGTP Collaborators. (2017). The Concise Guide to PHARMACOLOGY 2017/18: Other proteins. *British Journal of Pharmacology*, 174, S1–S16. <https://doi.org/10.1111/bph.13882>
- Alexander, S. P. H., Roberts, R. E., Broughton, B. R. S., Sobey, C. G., George, C. H., & Stanford, S. C. (2018). Goals and practicalities of immunoblotting and immunohistochemistry: A guide for submission to the British Journal of Pharmacology. *Br J Pharmacol* 175: 407–411.
- Atiya Ali, M., Poortvliet, E., Strömberg, R., & Yngve, A. (2011). Polyamines in foods: Development of a food database. *Food & Nutrition Research*, 55, 5572. <https://doi.org/10.3402/fnr.v55i0.5572>
- Beauloye, C., Bertrand, L., Horman, S., & Hue, L. (2011). AMPK activation, a preventive therapeutic target in the transition from cardiac injury to heart failure. *Cardiovascular Research*, 90(2), 224–233. <https://doi.org/10.1093/cvr/cvr034>
- Chen, O., Ye, Z., Cao, Z., Manaenko, A., Ning, K., Zhai, X., ... Sun, X. (2016). Methane attenuates myocardial ischemia injury in rats through anti-oxidative, anti-apoptotic and anti-inflammatory actions. *Free Radical Biology & Medicine*, 90, 1–11. <https://doi.org/10.1016/j.freeradbiomed.2015.11.017>
- Cheng, K., Malliaras, K., Shen, D., Tseliou, E., Ionta, V., Smith, J., ... Marbán, E. (2012). Intramyocardial injection of platelet gel promotes endogenous repair and augments cardiac function in rats with myocardial infarction. *Journal of the American College of Cardiology*, 59(3), 256–264. <https://doi.org/10.1016/j.jacc.2011.10.858>
- Curtis, M. J., Alexander, S., Cirino, G., Docherty, J. R., George, C. H., Giembycz, M. A., ... Ahluwalia, A. (2018). Experimental design and analysis and their reporting II: updated and simplified guidance for authors and peer reviewers. *British Journal of Pharmacology*, 175, 987–993. <https://doi.org/10.1111/bph.14153>
- Daskalopoulos, E., Dufey, C., Beauloye, C., Bertrand, L., & Horman, S. (2016). AMPK in cardiovascular diseases. *EXS*, 107, 179–201. https://doi.org/10.1007/978-3-319-43589-3_8
- Eisenberg, T., Abdellatif, M., Schroeder, S., Primessnig, U., Stekovic, S., Pendl, T., ... Madeo, F. (2016). Cardioprotection and lifespan extension by the natural polyamine spermidine. *Nature Medicine*, 22(12), 1428–1438. <https://doi.org/10.1038/nm.4222>
- Eisenberg, T., Knauer, H., Schauer, A., Büttner, S., Ruckenstein, C., Carmona-Gutierrez, D., ... Madeo, F. (2009). Induction of autophagy by spermidine promotes longevity. *Nature Cell Biology*, 11(11), 1305–1314. <https://doi.org/10.1038/ncb1975>
- Filippone, S., Samidurai, A., Roh, S., Cain, C., He, J., Salloum, F., ... Das, A. (2017). Reperfusion therapy with rapamycin attenuates myocardial infarction through activation of AKT and ERK. *Oxidative Medicine and Cellular Longevity*, 2017, 4619720.
- Francis Stuart, S., De Jesus, N., Lindsey, M., & Ripplinger, C. (2016). The crossroads of inflammation, fibrosis, and arrhythmia following myocardial infarction. *Journal of Molecular and Cellular Cardiology*, 91, 114–122. <https://doi.org/10.1016/j.yjmcc.2015.12.024>
- Fu, S., Chen, L., Wu, Y., Tang, Y., Tang, L., Zhong, Y., ... Chen, A. (2018). Gastrodin pretreatment alleviates myocardial ischemia/reperfusion injury through promoting autophagic flux. *Biochemical and Biophysical Research Communications*, 503(4), 2421–2428. <https://doi.org/10.1016/j.bbrc.2018.06.171>
- Galluzzi, L., Pietrocola, F., Levine, B., & Kroemer, G. (2014). Metabolic control of autophagy. *Cell*, 159(6), 1263–1276. <https://doi.org/10.1016/j.cell.2014.11.006>
- García-Prat, L., Martínez-Vicente, M., Perdiguer, E., Ortet, L., Rodríguez-Ubreva, J., Rebollo, E., ... Muñoz-Cánoves, P. (2016). Autophagy maintains stemness by preventing senescence. *Nature*, 529(7584), 37–42. <https://doi.org/10.1038/nature16187>
- Gottlieb, R. A., & Gustafsson, A. B. (2011). Mitochondrial turnover in the heart. *Biochimica et Biophysica Acta*, 1813(7), 1295–1301.
- Gupta, V., Scheunemann, L., Eisenberg, T., Mertel, S., Bhukel, A., Koemans, T., ... Sigrist, S. J. (2013). Restoring polyamines protects from age-induced memory impairment in an autophagy-dependent manner. *Nature Neuroscience*, 16(10), 1453–1460. <https://doi.org/10.1038/nn.3512>
- Ha, J., & Kim, J. (2016). Novel pharmacological modulators of autophagy: An updated patent review (2012–2015). *Expert Opinion on Therapeutic Patents*, 26(11), 1273–1289. <https://doi.org/10.1080/13543776.2016.1217996>
- Harding, S., Sharman, J., Faccenda, E., Southan, C., Pawson, A., Ireland, S., ... NC-IUPHAR (2018). The IUPHAR/BPS guide to pharmacology in 2018: Updates and expansion to encompass the new guide to immunopharmacology. *Nucleic Acids Research*, 46(D1), D1091–D1106. <https://doi.org/10.1093/nar/gkx1121>
- Hernández, J., Barreto-Torres, G., Kuznetsov, A., Khuchua, Z., & Javadov, S. (2014). Crosstalk between AMPK activation and angiotensin II-induced hypertrophy in cardiomyocytes: The role of mitochondria. *Journal of Cellular and Molecular Medicine*, 18(4), 709–720.
- Heusch, G., Libby, P., Gersh, B., Yellon, D., Böhm, M., Lopaschuk, G., & Opie, L. (2014). Cardiovascular remodelling in coronary artery disease and heart failure. *Lancet*, 383(9932), 1933–1943. [https://doi.org/10.1016/S0140-6736\(14\)60107-0](https://doi.org/10.1016/S0140-6736(14)60107-0)
- Hori, M., & Nishida, K. (2009). Oxidative stress and left ventricular remodelling after myocardial infarction. *Cardiovascular Research*, 81(3), 457–464.
- Hu, J., Cheng, P., Huang, G., Cai, G., Lian, F., Wang, X., & Gao, S. (2018). Effects of Xin-Ji-Er-Kang on heart failure induced by myocardial infarction: Role of inflammation, oxidative stress and endothelial dysfunction. *Phytomedicine*, 42, 245–257. <https://doi.org/10.1016/j.phymed.2018.03.036>
- Igarashi, K., & Kashiwagi, K. (2010). Modulation of cellular function by polyamines. *The International Journal of Biochemistry & Cell Biology*, 42(1), 39–51. <https://doi.org/10.1016/j.biocel.2009.07.009>
- Jernberg, T., Hasvold, P., Henriksson, M., Hjelm, H., Thuresson, M., & Janzon, M. (2015). Cardiovascular risk in post-myocardial infarction patients: Nationwide real world data demonstrate the importance of a long-term perspective. *European Heart Journal*, 36(19), 1163–1170. <https://doi.org/10.1093/eurheartj/ehu505>
- Kanamori, H., Takemura, G., Goto, K., Tsujimoto, A., Ogino, A., Takeyama, T., ... Minatoguchi, S. (2013). Resveratrol reverses remodeling in hearts with large, old myocardial infarctions through enhanced autophagy-activating AMP kinase pathway. *The American Journal of Pathology*, 182(3), 701–713. <https://doi.org/10.1016/j.ajpath.2012.11.009>
- Kilkenny, C., Browne, W., Cuthill, I. C., Emerson, M., & Altman, D. G. (2010). Animal research: Reporting in vivo experiments: The ARRIVE guidelines. *Journal of Gene Medicine*, 12(7), 561–563. <https://doi.org/10.1002/jgm.1473>
- Knott, A., & Bossy-Wetzel, E. (2010). Impact of nitric oxide on metabolism in health and age-related disease. *Diabetes, Obesity & Metabolism*, 12(Suppl 2), 126–133. <https://doi.org/10.1111/j.1463-1326.2010.01267.x>

- Kroemer, G., & Levine, B. (2008). Autophagic cell death: The story of a misnomer. *Nature Reviews. Molecular Cell Biology*, 9(12), 1004–1010. <https://doi.org/10.1038/nrm2529>
- LaRocca, T., Gioscia-Ryan, R., Hearon, C., & Seals, D. (2013). The autophagy enhancer spermidine reverses arterial aging. *Mechanisms of Ageing and Development*, 134(7–8), 314–320. <https://doi.org/10.1016/j.mad.2013.04.004>
- Ling, Y., Chen, G., Deng, Y., Tang, H., Ling, L., Zhou, X., ... Chen, A. (2016). Polydatin post-treatment alleviates myocardial ischaemia/reperfusion injury by promoting autophagic flux. *Clinical Science*, 130(18), 1641–1653. <https://doi.org/10.1042/CS20160082>
- Ma, X., Liu, H., Foyil, S., Godar, R., Weinheimer, C., & Diwan, A. (2012). Autophagy is impaired in cardiac ischemia-reperfusion injury. *Autophagy*, 8(9), 1394–1396. <https://doi.org/10.4161/auto.21036>
- Madeo, F., Eisenberg, T., Pietrocola, F., & Kroemer, G. (2018). Spermidine in health and disease. *Science*, 359(6374), eaan2788. <https://doi.org/10.1126/science.aan2788>
- McGrath, J. C., Drummond, G. B., McLachlan, E. M., Kilkenny, C., & Wainwright, C. L. (2010). Guidelines for reporting experiments involving animals: The ARRIVE guidelines. *British Journal of Pharmacology*, 160, 1573–1576. <https://doi.org/10.1111/j.1476-5381.2010.00873.x>
- McGrath, J. C., & Lilley, E. (2015). Implementing guidelines on reporting research using animals (ARRIVE etc.): new requirements for publication in BJP. *Br J Pharmacol*, 172, 3189–3193.
- McMurray, J. (2011). Consensus to emphasis: The overwhelming evidence which makes blockade of the renin-angiotensin-aldosterone system the cornerstone of therapy for systolic heart failure. *European Journal of Heart Failure*, 13, 929–936. <https://doi.org/10.1093/eurjhf/hfr093>
- Meana, C., Rubin, J., Bordallo, C., Suárez, L., Bordallo, J., & Sánchez, M. (2016). Correlation between endogenous polyamines in human cardiac tissues and clinical parameters in patients with heart failure. *Journal of Cellular and Molecular Medicine*, 20(2), 302–312. <https://doi.org/10.1111/jcmm.12674>
- Michiels, C., Kurdi, A., Timmermans, J., De Meyer, G., & Martinet, W. (2016). Spermidine reduces lipid accumulation and necrotic core formation in atherosclerotic plaques via induction of autophagy. *Atherosclerosis*, 251, 319–327. <https://doi.org/10.1016/j.atherosclerosis.2016.07.899>
- Milovic, V. (2001). Polyamines in the gut lumen: Bioavailability and biodistribution. *European Journal of Gastroenterology & Hepatology*, 13(9), 1021–1025. <https://doi.org/10.1097/00042737-200109000-00004>
- Murray, C., & Lopez, A. (1997). Mortality by cause for eight regions of the world: Global Burden of Disease Study. *Lancet*, 349(9061), 1269–1276. [https://doi.org/10.1016/S0140-6736\(96\)07493-4](https://doi.org/10.1016/S0140-6736(96)07493-4)
- Nian, M., Lee, P., Khaper, N., & Liu, P. (2004). Inflammatory cytokines and postmyocardial infarction remodeling. *Circulation Research*, 94(12), 1543–1553. <https://doi.org/10.1161/01.RES.0000130526.20854.f4>
- Noppe, G., Dufey, C., Buchlin, P., Marquet, N., Castaneres-Zapatero, D., Balteau, M., ... Horman, S. (2014). Reduced scar maturation and contractility lead to exaggerated left ventricular dilation after myocardial infarction in mice lacking AMPK α 1. *Journal of Molecular and Cellular Cardiology*, 74, 32–43. <https://doi.org/10.1016/j.yjmcc.2014.04.018>
- Pegg, A. (2016). Functions of polyamines in mammals. *The Journal of Biological Chemistry*, 291(29), 14904–14912. <https://doi.org/10.1074/jbc.R116.731661>
- Sansbury, B., DeMartino, A., Xie, Z., Brooks, A., Brainard, R., Watson, L., ... Hill, B. G. (2014). Metabolomic analysis of pressure-overloaded and infarcted mouse hearts. *Circulation. Heart Failure*, 7(4), 634–642. <https://doi.org/10.1161/CIRCHEARTFAILURE.114.001151>
- Soda, K., Kano, Y., Sakuragi, M., Takao, K., Lefor, A., & Konishi, F. (2009). Long-term oral polyamine intake increases blood polyamine concentrations. *Journal of Nutritional Science and Vitaminology*, 55(4), 361–366. <https://doi.org/10.3177/jnsv.55.361>
- Sun, D., & Yang, F. (2017). Metformin improves cardiac function in mice with heart failure after myocardial infarction by regulating mitochondrial energy metabolism. *Biochemical and Biophysical Research Communications*, 486(2), 329–335. <https://doi.org/10.1016/j.bbrc.2017.03.036>
- Sun, L., Zhang, S., Yu, C., Pan, Z., Liu, Y., Zhao, J., ... Li, Y. (2015). Hydrogen sulfide reduces serum triglyceride by activating liver autophagy via the AMPK-mTOR pathway. *American Journal of Physiology. Endocrinology and Metabolism*, 309(11), E925–E935. <https://doi.org/10.1152/ajpendo.00294.2015>
- Tannous, P., Zhu, H., Nemchenko, A., Berry, J., Johnstone, J., Shelton, J., ... Hill, J. A. (2008). Intracellular protein aggregation is a proximal trigger of cardiomyocyte autophagy. *Circulation*, 117(24), 3070–3078. <https://doi.org/10.1161/CIRCULATIONAHA.107.763870>
- White, H., Norris, R., Brown, M., Brandt, P., Whitlock, R., & Wild, C. (1987). Left ventricular end-systolic volume as the major determinant of survival after recovery from myocardial infarction. *Circulation*, 76(1), 44–51. <https://doi.org/10.1161/01.CIR.76.1.44>
- Yang, Y., Chen, S., Zhang, Y., Lin, X., Song, Y., Xue, Z., ... Zhang, L. (2017). Induction of autophagy by spermidine is neuroprotective via inhibition of caspase 3-mediated Beclin 1 cleavage. *Cell Death & Disease*, 8(4), e2738. <https://doi.org/10.1038/cddis.2017.161>
- Zhang, Y., Ling, Y., Yang, L., Cheng, Y., Yang, P., Song, X., ... Wang, X. (2017). Liraglutide relieves myocardial damage by promoting autophagy via AMPK-mTOR signaling pathway in Zucker diabetic fatty rat. *Molecular and Cellular Endocrinology*, 448, 98–107. <https://doi.org/10.1016/j.mce.2017.03.029>
- Zheng, Z., Wang, Z., Chen, Y., Chen, J., Khor, S., Li, J., ... Wang, X. (2018). Spermidine promotes nucleus pulposus autophagy as a protective mechanism against apoptosis and ameliorates disc degeneration. *Journal of Cellular and Molecular Medicine*, 22(6), 3086–3096. <https://doi.org/10.1111/jcmm.13586>
- Zhong, Y., Zhong, P., He, S., Zhang, Y., Tang, L., Ling, Y., ... Wang, X. (2017). Trimetazidine protects cardiomyocytes against hypoxia/reoxygenation injury by promoting AMP-activated protein kinase-dependent autophagic flux. *Journal of Cardiovascular Pharmacology*, 69(6), 389–397. <https://doi.org/10.1097/FJC.0000000000000487>
- Zoumas-Morse, C., Rock, C., Quintana, E., Neuhauser, M., Gerner, E., & Meyskens, F. (2007). Development of a polyamine database for assessing dietary intake. *Journal of the American Dietetic Association*, 107(6), 1024–1027. <https://doi.org/10.1016/j.jada.2007.03.012>

SUPPORTING INFORMATION

Additional supporting information may be found online in the Supporting Information section at the end of the article.

How to cite this article: Yan J, Yan J-Y, Wang Y-X, et al. Spermidine-enhanced autophagic flux improves cardiac dysfunction following myocardial infarction by targeting the AMPK/mTOR signalling pathway. *Br J Pharmacol*. 2019;176: 3126–3142. <https://doi.org/10.1111/bph.14706>